Experimental Investigation of Fillet-Welded Joints Subjected to Out-of-Plane Eccentric Loads

AMIT M. KANVINDE, GILBERT Y. GRONDIN, IVAN R. GOMEZ and YUKAY KWAN

Fillet-welded connections are popular in civil engineering construction due to their economy (minimal surface preparation is required prior to welding) and strength, and various aspects of their response have been studied extensively over the past five decades. Building on the early studies of Ligtenburg (1968), Clark (1971) and Butler and Kulak (1971), subsequent research efforts (e.g., Butler, Pal and Kulak, 1972; Miazga and Kennedy, 1986, 1989; Lesik and Kennedy, 1990) have led to the development of strength prediction approaches for welded connections loaded concentrically as well as eccentrically. Design considerations based on these approaches have been implemented in current North American design specifications (AISC, 2005; CISC, 2007).

Within this overall theme of research on fillet-welded connections, this paper focuses on the response of eccentrically loaded fillet welds where the load is not in the plane of the weld group, such as illustrated schematically in Figure 1(a). This type of weld group and loading configuration is described as a "special-case" in current weld design tables provided by the American Institute of Steel Construction (Table 8-4, *Steel Construction Manual*, AISC, 2005). Referring to the illustration in Figure 1(a), these joints resist the applied load through the development of stresses in the welds as well as bearing stresses over the contact surface of the attached plates. However, as discussed in this and the subsequent section, approaches adopted in current design practice (AISC, 2005) do not incorporate all aspects of behavior that control the strength of these joints. The design table adopted by AISC (Table 8-4, *Steel Construction Manual*, AISC, 2005) is based on the method of the instantaneous center (IC) of rotation (Tide, 1980). This IC method, as applied in development of the current design table, relies on the principle that at the strength limit state, the weld group rotates about a center of rotation, resulting in compatible deformations for all segments of the weld. Contingent on these deformations, the stresses in the weld segments are determined through a load-deformation relationship such as the one proposed by Lesik and Kennedy (1990). While the assumptions underlying the design table are consistent with the response of eccentrically loaded lap joints, they are questionable when applied to eccentrically loaded joints where the applied load is not in the plane of the weld group. Specifically, two issues are of concern. First, the eccentrically loaded configuration shown in Figure 1(a) produces a root notch at the unfused interface of the plates. Previous studies (e.g., Ng et al., 2002; Pham, 1983; Kanvinde et al., 2008) indicate that such a root notch, perpendicular to the direction of the bending stresses in the connection, produces a crack-like effect, possibly reducing both the strength and the ductility of the welds with respect to values implicitly assumed in the design table. This flaw, subjected to Mode I (crack opening) loads, is of greater concern as compared to a similar flaw in lap joints, which is subjected to Mode II (shear) loads. The second, and perhaps a more important issue, pertains to bearing in the region of compression between the connected plates. The design table is based on an approach that disregards this effect (Tide, 1980), leading to an inappropriate representation of the stress distribution in the welded joint. The reliance on this approach may be due to the relative lack of experimental data from welds loaded eccentrically out of plane. In fact, in addition to the current study, only two other documented test programs

Amit M. Kanvinde is an assistant professor of civil and environmental engineering, University of California, Davis.

Gilbert Y. Grondin is a professor of civil and environmental engineering, University of Alberta, Edmonton.

Ivan R. Gomez is a graduate student researcher in civil and environmental engineering, University of California, Davis.

YuKay Kwan is a graduate student researcher in civil and environmental engineering, University of Alberta, Edmonton.

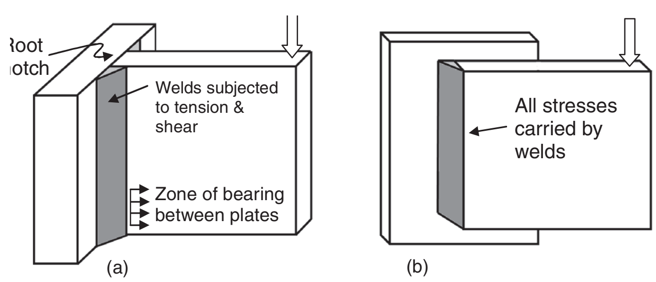

Fig. 1. Welded connection subjected to (a) out-of-plane eccentric load and (b) in-plane eccentric load.

(Dawe and Kulak, 1972, 1974; Beaulieu and Picard, 1985) have investigated this situation experimentally. Motivated by these issues, the main objectives of this paper are to (1) obtain a data set of test results of sufficient size to conduct a meaningful statistical analysis of the strength characteristics of welded connections loaded with out-of-plane eccentricity, (2) evaluate the effect of various parameters (under a wider range of values) on this strength in a systematic way, and (3) assess the applicability and level of safety provided by current design practice.

To realize these objectives, the main experimental basis for this paper is a series of 60 bend tests on cruciform specimens (such as shown in Figure 2) that evaluate the effect of a range of parameters, including weld size, weld metal toughness, load eccentricity and plate bearing width. The tests presented here are part of a comprehensive parent study that also included experiments and investigations of the effect of the weld root notch on the tensile strength and ductility of fillet welds (Gomez et al., 2008).

A review of the literature relevant to this study is first presented. Subsequent sections address the experimental program, including ancillary tests and bending tests on cruciform welded specimens to investigate the out-of-plane loading condition. The data from these tests are then reviewed and analyzed along with data from prior testing programs to assess the effectiveness of the current design approach and the effect of various parameters on its applicability. An alternate model that considers the bearing effect between the plates is presented as a more suitable method to characterize the joint strength. The paper concludes by reviewing the findings and limitations of the study while outlining strategies for future research.

BACKGROUND AND OBJECTIVES

This section summarizes prior research from the early 1970s to the present, focusing on the development of test programs and analysis methods of the behavior of fillet-welded joints with out-of-plane eccentricity. While the review presented here is directly relevant to this paper, a more comprehensive background of related research (including studies on various weld configurations under concentric loading) is available in Gomez et al. (2008) and Ng et al. (2002).

Several experimental studies (e.g., Butler et al., 1972; Swannell, 1981a, 1981b; Sanaei and Kamtekar, 1988) have investigated the behavior of eccentrically loaded fillet-welded connections through experiments on lapped specimens, such as illustrated schematically in Figure 1(b). Whereas these studies have validated several theoretical approaches to predict the strength of these eccentrically loaded welded connections, they only consider situations where the eccentric load is in the plane of the weld group, such as illustrated in Figure 1(b). Experimental studies that examine situations where the eccentric load is not in the plane of the weld group, such as illustrated in Figure 1(a), are relatively scarce, and prior to the current study, only two significant documented test projects have investigated this configuration. These are reviewed first, before discussing various theoretical models for strength prediction.

The first experimental study, by Dawe and Kulak (1972), included eight specimens to investigate the behavior of weld groups subjected to out-of-plane eccentric loading. The test specimens consisted of a wide flange section with its end welded to an end plate by fillet welds along the outer side of each flange. The test configuration involved loading the wide flange sections in minor axis bending to determine the joint strength. The key variables investigated included the length of weld, the eccentricity of load and the thickness of the connected plate. Two nominal weld lengths (8 in. and 12 in.) and four load eccentricities (ranging from 8 in. to 20 in.) were considered. Since the specimens were loaded in the minor axis orientation, the effective plate bearing width was determined as twice the flange thickness of the wide flange section. Using this interpretation, five nominal bearing widths (ranging from 0.86 in. to 1.24 in.) were investigated. All specimens were fabricated from ASTM A36 steel and featured ¼-in. (nominal leg size) fillet welds deposited with AWS A5.1 E60XX compliant electrodes. Table 1 summarizes the main aspects of the test series, including test results, which will be discussed later. A detailed analysis of these data and comparison to the current study are presented in a subsequent section.

The second experimental study, by Beaulieu and Picard (1985), included a total of 24 fillet welded plate connections loaded eccentrically out-of-plane. Referring to Table 1, the

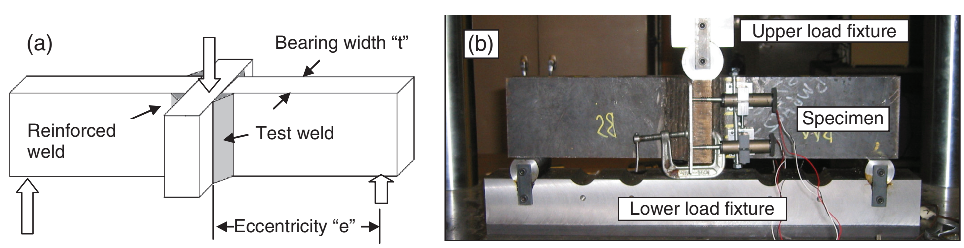

Fig. 2. Cruciform joint bending specimens: (a) schematic and (b) photograph of test setup.

Table 1. Results of Cruciform Bend Tests from Dawe and Kulak (1972) and Beaulieu and Picard (1985)

Test Program	Test #	a[a]	Nom[b] in.	t[c] in.	R_{max}[d] kips	$\dfrac{R_{max}}{R_n^{AISC}}$[e]	$\dfrac{R_{max}}{R_n^{bearing}}$[f]
Dawe and Kulak (1972)	1	1.03	¼	1.04	62.5	1.36	1.07
	2	1.53	¼	1.04	39.0	1.22	0.96
	3	2.03	¼	1.04	23.1	0.99	0.78
	4	2.56	¼	1.06	19.5	1.06	0.83
	5	2.04	¼	0.86	23.6	1.02	0.89
	6	2.02	¼	1.52	32.6	1.29	0.95
	7	1.26	¼	1.24	59.7	1.11	0.83
	8	1.69	¼	1.24	49.6	1.15	0.88
Beaulieu and Picard (1985)[g]	1	1.50	¼	0.79	50.9	1.08	1.02
	2	1.50	½	0.79	61.9	0.73	0.94
	3	0.50	¼	0.79	157.9	1.19	1.10
	4	0.50	¼	0.79	141.7	1.10	1.00
	5	0.30	¼	0.79	245.9	1.39	1.27
	6	1.51	⁵⁄₁₆	1.58	93.5	1.27	1.03
	7	1.49	⁵⁄₁₆	1.58	96.1	1.31	1.05
	8	1.51	⅜	1.58	61.3	0.85	0.68
	9	1.51	⅜	1.58	109.1	1.49	1.20
	10	0.50	⁵⁄₁₆	1.58	235.7	1.35	1.08
	11	0.50	⁵⁄₁₆	1.58	286.6	1.66	1.32
	12	0.50	⅜	1.58	266.2	1.56	1.24
	13	0.50	⅜	1.58	249.5	1.39	1.12
	14	0.30	⁵⁄₁₆	1.58	334.6	1.68	1.45
	15	0.30	⁵⁄₁₆	1.58	313.4	1.66	1.43
	16	0.31	⅜	1.58	381.5	1.42	1.24
	17	0.30	⅜	1.58	358.7	1.34	1.18
					Mean	**1.27**	**1.06**
					Coefficient of variation	**0.19**	**0.19**

[a] Load eccentricity ratio = load eccentricity length divided by weld group length.
[b] Nominal (specified) weld size.
[c] Plate (root notch) thickness.
[d] R_{max} = maximum eccentric force observed in experiments.
[e] R_n^{AISC} = predicted strength based on AISC approach.
[f] $R_n^{bearing}$ = predicted strength on alternate approach incorporating bearing.
[g] Only 17 of 24 tests reported; others failed by plate rupture.

key variables investigated in this study include the weld size (nominally ¼ in., ⅜ in., ⁵⁄₁₆ in. and ½ in.), the load eccentricity (ranging between 3 in. and 14.75 in.) and the bearing width, also equal to the root notch length (0.787 in. and 1.575 in.). All specimens were fabricated from ASTM A36 steel, and the welds (all approximately 10 in. long) were deposited using AWS A5.1 E70XX electrodes. The 17 experiments included in Table 1 represent only those that exhibited weld failure and do not include other specimens that showed base metal failure due to tearing.

Building on these and other studies on lap-joint specimens (such as those briefly mentioned earlier), various theoretical methods have been proposed to determine the strength of eccentrically loaded fillet welds. Broadly, these may be classified into three categories: (1) methods that assume elastic response of all the welds, (2) methods that apply the principle of the instantaneous center (IC) of rotation, and (3) methods that assume a predetermined form of the stress distribution in the welds and in the bearing portion of the connected plates. The elastic methods are generally understood to be highly conservative (Lesik and Kennedy, 1990; Salmon and Johnson, 1996), while those that apply the principle of the IC of rotation and an assumed stress distribution reflect more realistic response, including inelastic action in the welds. With this background, this section reviews the development of these methods.

Butler et al. (1972) developed a method to predict the strength of welded joints with in-plane eccentricity based on the approach previously proposed by Crawford and Kulak (1971) for eccentrically loaded bolted joints. This method employs the load deformation response of weld elements as a function of loading angle and relies on the assumption that the weld group, under an eccentric load, rotates about an instantaneous center of rotation. Once the location of the IC is established (through an iterative process until equilibrium of forces and moments is satisfied), the strength of the joint is calculated considering equilibrium of all the weld elements when the critical element (typically farthest from the IC) reaches its ultimate (or fracture) deformation. Various aspects of this method have been refined in subsequent years, including load-deformation relationships of the weld elements themselves, which is an important input to these methods. The original work of Butler et al. (1971) was based on a load-deformation model for fillet welds based on a series of tests on ¼-in. welds conducted by Butler and Kulak (1971). Lesik and Kennedy (1990) subsequently refined the load-deformation models based on the tests of Miazga and Kennedy (1986, 1989) on double-lapped connections. The IC method has also been adapted for eccentrically loaded joints loaded out-of-plane, where plate bearing in the compression zone may alter the stress distribution in the welds (Dawe and Kulak, 1972).

Neis (1980) simplified the ultimate weld capacity prediction procedures proposed by Dawe and Kulak (1972). The model presented by Neis assumes a stress distribution in the weld adopted from the research of Butler and Kulak (1971) for a weld loaded perpendicular to its axis ($\theta = 90°$). This approach obviates the iterative procedures typically involved in the IC methods and obtains predictions as a closed-form solution. Neis suggested seven variants of the model, which featured various combinations of stress block geometries for the welds and assumptions regarding bearing stress distribution in the compression zone. Beaulieu and Picard (1985) presented a model similar to Neis (1980) by assuming that the bearing strength is equal to the yield strength of the bearing plates. Both Neis (1980) and Beaulieu and Picard (1985) neglect shear stresses in the welds and are valid only for relatively large load eccentricities (ratio of eccentricity to weld length greater than 0.4).

The American Institute of Steel Construction (AISC, 2005) published tables (*Steel Construction Manual*, Table 8-4, "special-case") for the strength of eccentric fillet welded connections loaded out-of-plane. Figure 3 schematically illustrates the assumptions and stress distributions reflected in the AISC design tables. As indicated in the figure, the stresses in the welds are based on the IC method employing the descriptions of the fillet weld load-deformation response proposed by Lesik and Kennedy (1990). Lesik and Kennedy performed extensive analysis on test data of Miazga and Kennedy (1986, 1989) to provide algebraic expressions for the load-deformation relationships of fillet welds. As per their research, for a weld segment of leg size w and unit length (such as indicated in Figure 3) loaded at an angle θ with respect to its axis, the load-deformation relationship may be expressed as follows:

$$f(\rho) = 8.234\rho \text{ for } 0 < \rho \leq 0.0325 \tag{1}$$

$$\begin{aligned} f(\rho) = &-13.29\rho + 457.32\rho^{1/2} - 3385.9\rho^{1/3} \\ &+ 9054.29\rho^{1/4} - 9952.13\rho^{1/5} \\ &+ 3840.71\rho^{1/6} \text{ for } \rho > 0.0325 \end{aligned} \tag{2}$$

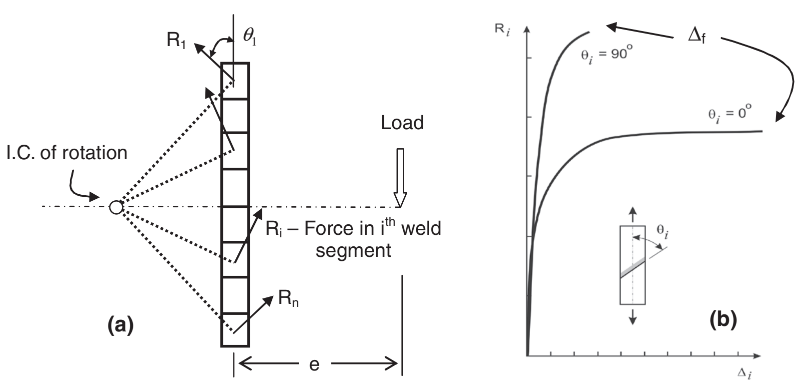

Fig. 3. Assumptions inherent in the AISC design tables: (a) weld deformation and stresses, (b) load deformation response of welds (Lesik and Kennedy, 1990).

where $f(\rho)$ is the normalized force in the i^{th} weld element, such that $f(\rho) = R_i/R_{ult}$, and:

$$R_{ult} = 0.60F_{EXX}\,A_w(1.0 + 0.5\sin^{1.5}\theta) \tag{3}$$

Equation 3 predicts the capacity of a fillet weld segment in terms of the electrode nominal tensile strength, F_{EXX}, the weld throat area, A_w, and the angle, θ, between the axis of the weld and the line of action of the force. The constant 0.60 is the shear stress transformation factor. The deformation quantity described in Equations 1 and 2 is normalized by the deformation at peak force such that $\rho = \Delta/\Delta_u$, where:

$$\Delta_u = 0.209(\theta + 2)^{-0.32w} \tag{4}$$

As per the IC method (Butler et al., 1972), the weld group is assumed to rotate until a critical segment (typically farthest from the IC) reaches its fracture deformation, Δ_f, which is determined as follows:

$$\Delta_f = 1.087D(\theta + 6)^{-0.65w} \le 0.17_w \tag{5}$$

At this point, the equilibrium of the entire connection is considered, and the force capacity is determined. Referring to the preceding discussion and Figure 3, some of the assumptions implicit in the formulation of the AISC design tables are questionable. For example, the weld load-deformation response described by Equations 1 through 5 is based on tests of lap-joint specimens. Thus, the equations (especially Equation 5 which reflects weld fracture deformation) neglect the crack-like effect of the root notch, as shown in Figure 1(a), which may potentially impact weld strength and ductility. In this context, it is relevant to mention recent tests by Ng et al. (2002), Li et al. (2007) and Kanvinde et al. (2008) on welded cruciform joint specimens, which indicate that the ductility (and to some extent the strength) of welds is diminished when the load is applied perpendicular to the root notch. Perhaps more importantly, the approach disregards bearing between the two connected plates in the compression region and assumes that all the stresses are carried by the welds (refer to Figure 3). Thus, the actual behavior of the welds for out-of-plane loading is not reflected by the AISC approach.

In summary, prior research features limited test data with respect to eccentric weld connections loaded out-of-plane. Thus, the theoretical methods to predict the strength cannot be evaluated for a wide range of parameters. The methods themselves are based on several assumptions, outlined in the preceding discussion. Moreover, since all the methods are based on weld load-deformation relationships derived from tests on lap-joint specimens, none consider the potentially detrimental effect of the root notch on the ductility of the welds. Finally, an examination of current AISC design tables indicates that significant aspects of physical response, such as bearing between the connected plates, are not considered in their development. To address these issues, the main objectives of the current study, as discussed in the introduction, are to evaluate the applicability of the current design standards to joints with out-of-plane eccentricity and to suggest improved alternatives.

ANCILLARY TESTS

A series of ancillary tests was conducted to characterize material properties in support of the cruciform joint bending tests. Described in the next section, the cruciform joint bend specimens were fabricated from ASTM A572 Grade 50 base metal, and two different types of E70XX weld filler metals (self shielded flux-cored wires), including an AWS A5.20 (2005a) E70T-7 electrode, which is designated as a "non-toughness-rated" filler metal, and a "toughness-rated" E70T7-K2 electrode per AWS A5.29 (AWS, 2005b). Welds designated "toughness-rated" meet minimum Charpy V-Notch toughness requirements of 27 joules at –29 °C and 54 joules at 21 °C. Standard tension tests (per AWS A5.20, 2005a, and AWS A5.29, 2005b, for welds; ASTM E8, 2008, for base metal) were conducted to characterize material constitutive response. The test method for the weld materials involved creating a groove-welded assembly of two plates per AWS 5.20 (2005a), shown schematically in Figure 4, from weld electrodes used for fabrication of the cruciform bend tests. Referring to the figure, all-weld metal specimens (two for each weld material) were extracted from the groove weld region and tested under monotonic tension. Average results from these tests, including the yield and ultimate strengths and ductilities expressed in terms of the ratio of pre- to post-fracture cross section diameter d_0/d_f (and the corresponding maximum true strains at fracture), are summarized in Table 2. The mean ultimate strengths $F_{u,\,weld}$ (from quasi-static tests) for both the E70T-7 and E70T7-K2 weld metals are approximately 97 ksi, on average 40% greater than the specified minimum (70 ksi). As expected, the average ductility, d_0/d_f, for the toughness rated E70T7-K2 weld material is greater (by about 35%) as compared to the non-toughness-rated (E70T-7) weld material. Similar results from tension tests of the base metal are also

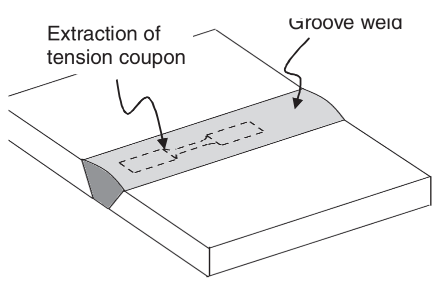

Fig. 4. Plate assembly (per AWS A5.20) indicating extraction of all-weld metal tension specimens.

Table 2. Results from Ancillary Tests Including Tension and Charpy V Notch Tests								
		Tension Tests				CVN Energy (lb-ft)		
Material	Test	F_y[a] ksi	F_u[b] ksi	d_o/d_f	ε[c]	–20 °F	70 °F	212 °F
E70T-7 (Non-toughness-rated weld)	1	75.8	97.1	1.35	0.60	5.5	19.0	41.0
	2	76.8	97.2	1.15	0.28	6.0	18.0	41.0
	Mean	**76.3**	**97.1**	**1.25**	**0.45**	**5.75**	**18.5**	**41.0**
E70T7-K2 (Toughness-rated weld)	1	82.7	97.5	1.65	1.00	30	56.0	88.0
	2	83.0	97.4	1.74	1.11	23	62.0	88.0
	Mean	**82.8**	**97.4**	**1.69**	**1.05**	**26.5**	**59.0**	**88.0**
A572 Grade 50 (Base metal)	1	52.9	71.5	2.13	1.52	CVN tests not conducted for base metal		
	2	53.9	71.8	2.08	1.46			
	Mean	**53.4**	**71.6**	**2.11**	**1.49**			

[a] Measured yield stress, based on 0.2% offset method; static value
[b] Measured ultimate strength; static value
[c] $\varepsilon = \ln(d_0/d_f)^2$ = average true strain across necked cross section of tension coupon

presented in Table 2. In addition to these mechanical tests, spectrochemical analyses were carried out for both weld metal electrodes. The analyses (archived in Roberts, 2008) indicate that none of the electrodes had an unexpected chemical composition relative to the requirements of AWS 5.20 (2005a).

Similar ancillary tests have been conducted for the other experimental programs (Dawe and Kulak, 1972; Beaulieu and Picard, 1985). Although these ancillary data are not reproduced in this paper (since they are available in the cited references), they are used in the analysis of bend test data from these programs.

EXPERIMENTAL PROGRAM

This section describes the cruciform joint bending tests in detail. Figure 2(a) illustrates the test setup and specimen schematically, whereas Figure 2(b) includes a photograph of a specimen being loaded in a three-point-bend configuration. The main variables investigated are (1) the load eccentricity, e; (2) the plate bearing width or plate thickness, t, which is also equal to the nominal root notch dimension; (3) weld size and (4) weld filler metal classification. Table 3 presents the test matrix indicating that three replicates are tested for each assembly (or test category) to obtain statistically significant data. Referring to the table, two nominal weld sizes (½ in. and 5⁄16 in. leg dimension), three load eccentricities (e = 3.0, 5.5 and 8.5 in.) and three plate widths (t = 1.25, 1.75 and 2.50 in.) were investigated for each of the two weld classifications. For economy, the test matrix represents a fractional factorial matrix; that is, not all possible parameter combinations are investigated explicitly. However, the matrix is designed to provide comparative evaluations of the effect of all parameters. The following discussion outlines the specimen preparation, test setup and procedure. Discussion of the test results is presented in a subsequent section.

Test Specimen Preparation and Test Setup

Figure 5 schematically illustrates the typical specimen geometry. As shown in the figure, for each configuration, three replicate specimens (nominally 4 in. wide) were cut out from an assembly of three plates (all A572 Grade 50 ksi steel) welded together in a cruciform configuration. The plate bearing width (i.e., the root notch length) was controlled by varying the thickness of the two outer plates. The connection was designed so that failure occurred in the test welds while the connecting plates remained elastic. The overall width of the assembly was 13 in. allowing run-on and run-off regions at either end of the assembly to ensure relatively uniform weld properties within each specimen. Each of the two filler metal types (E70T-7 and E70T7-K2) was taken from the same spool of wire to minimize variability in weld properties. Standard weld procedures (Roberts, 2008) were used, and all welding was performed using the flux cored arc welding (FCAW) process. Three weld passes were needed for the ½-in. welds, while only one pass was needed for the 5⁄16-in. welds. As indicated in Figure 5, one side of the central plate had reinforced welds (i.e., they were oversized by approximately ½ in.) to ensure failure on the predetermined "test" side, thereby minimizing instrumentation.

The loading fixture shown in Figure 2(b) was designed to enable testing of the cruciform joint specimens in bending with different load eccentricities, while also providing pinned boundary conditions. The fixture includes a steel base with smooth-cut round grooves (at multiple preset locations) in which dowel pins may be seated as the supports. A similar dowel pin is connected to the central (upper) loading fixture. All dowel pins feature a milled flat surface to minimize local deformations of the specimen at the reaction points. The round dowels were lubricated to allow free rotation at the contact points. The eccentricity for each test, as illustrated in Figure 2(a), is defined as the distance from the centerline of the dowel to the surface of the center plate.

Using the load setup and fixture described earlier, 60 cruciform specimens were loaded quasi-statically to failure under displacement control. Qualitatively, all tests exhibited a similar response: initial elastic response followed by a period of strain hardening concluding with a drop in force. Figure 6 shows a representative load versus load-line deformation curves for Test 8 (eccentricity = 3.0 in.) and Test 52 (eccentricity = 8.5 in.). The load shown in the figure is half the load applied at the center of the symmetric three-point-bend specimen, representing the force sustained by the test weld, which is located on one side of the central loading fixture. Failure for most tests with larger eccentricities (e = 5.5 in. and 8.5 in.) was gentle, and weld rupture involved a gradual “un-zipping” of the specimen initiating at the bottom end of the weld (the tension end); see the response of Test 52 shown in Figure 6. A majority of the tests with the smaller eccentricity (i.e. e = 3.0 in.) exhibited more sudden shearing failure, corresponding to an abrupt drop in load (see response of Test 8 shown in Figure 6). Figure 7(a) shows a fractured specimen (Test 19) photographed at the conclusion of testing. Several load and deformation quantities were measured during the tests, including the peak load, R_{max} (as indicated on Figure 6), the load line displacement, the weld deformation at four locations and, in some specimens, the longitudinal surface strains. While a detailed discussion of these various quantities is presented in Gomez et al. (2008), the observed peak load, R_{max} (or connection strength), is most relevant in the context of this paper. Table 3 summarizes measured R_{max} values for all the test specimens, along with other quantities. A discussion of these results along with a graphical representation is presented in a subsequent section.

Pre- and Post-Fracture Specimen Measurements

To minimize systematic bias in the analysis of the test data, detailed measurements of the weld sizes were recorded both before and after testing. The profiles of all the test welds

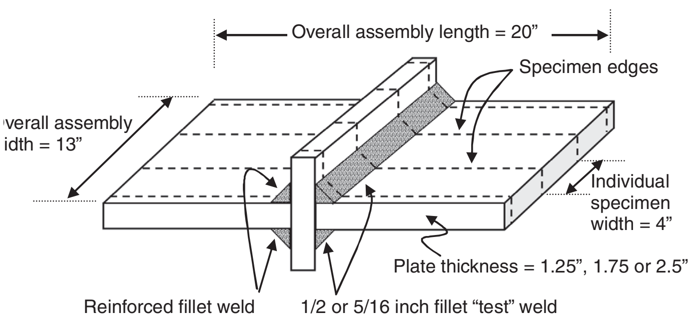

Fig. 5. Cruciform specimen assembly showing key dimensions and fabrication details.

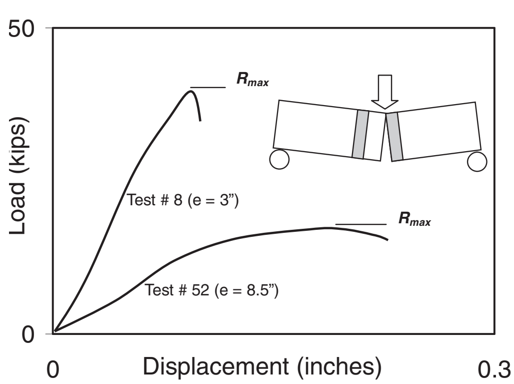

Fig. 6. Representative load-deformation curve for Test 8 and Test 52 (indicating the peak load, R_{max}).

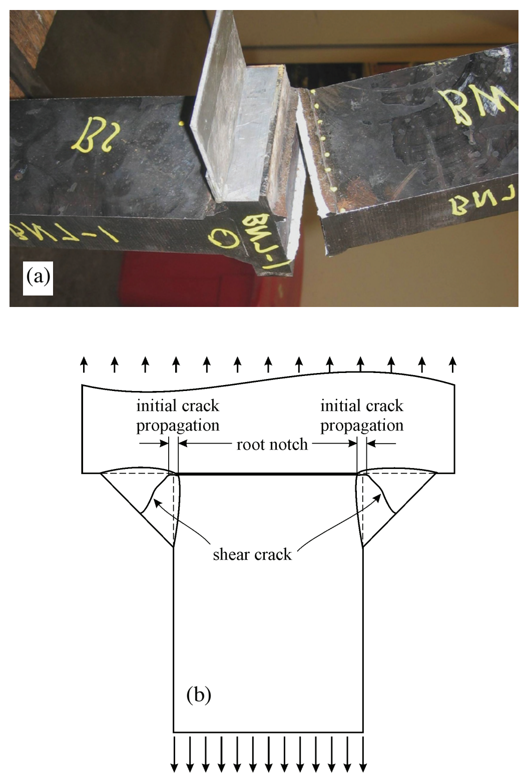

Fig. 7. (a) Representative photograph of failed specimen (Test 19); (b) schematic bottom view of specimen indicating failure pattern.

Test No.[a] NT	Test No.[a] T	e[b] in.	Weld Size (in.) Nom[c]	Weld Size (in.) w_{eff}[d] NT	Weld Size (in.) w_{eff}[d] T	t[e] in.	R_{max}[f] kips NT	R_{max}[f] kips T	R_{max}/R_n^{AISC}[g] NT	R_{max}/R_n^{AISC}[g] T	$R_{max}/R_n^{bearing}$[h] NT	$R_{max}/R_n^{bearing}$[h] T
1	31	5.5	5/16	0.400	0.427	1.25	44.4	50.5	1.41	1.58	1.19	1.36
2	32			0.399	0.426		53.7	57.4	1.68	1.75	1.42	1.50
3	33			0.411	0.421		52.5	60.8	1.63	1.95	1.39	1.67
4	34		1/2	0.593	0.589		73.4	82.0	1.55	1.66	1.55	1.65
5	35			0.591	0.562		72.2	84.5	1.50	1.84	1.49	1.78
6	36			0.587	0.608		71.1	98.8	1.46	1.84	1.45	1.86
7	37	3.0	5/16	0.359	0.403	1.75	120.0	165.2	2.34	2.79	1.73	2.12
8	38			0.365	0.382		119.0	160.4	2.23	2.71	1.66	2.04
9	39			0.361	0.387		123.9	155.3	2.26	2.64	1.68	1.99
10	40		1/2	0.551	0.583		153.4	193.2	2.02	2.17	1.68	1.84
11	41			0.555	0.580		175.0	200.0	2.14	2.30	1.79	1.94
12	42			0.570	0.563		152.1	185.4	1.94	2.17	1.63	1.81
13	43	5.5	5/16	0.367	0.445		61.7	86.7	1.95	2.31	1.42	1.80
14	44			0.366	0.424		59.7	69.8	1.90	1.94	1.39	1.50
15	45			0.371	0.360		63.0	78.0	2.08	2.53	1.52	1.84
16	46		1/2	0.598	0.583		90.0	99.3	1.73	2.02	1.48	1.72
17	47			0.563	0.602		76.6	90.0	1.79	1.91	1.50	1.65
18	48			0.584	0.574		79.6	86.6	1.71	1.92	1.46	1.62
19	49	8.5	5/16	0.418	0.419		39.0	45.9	1.81	1.92	1.38	1.45
20	50			0.422	0.416		30.1	46.8	1.43	2.08	1.09	1.58
21	51			0.417	0.418		33.4	46.0	1.53	2.04	1.16	1.54
22	52		1/2	0.585	0.588		51.9	59.3	1.57	1.78	1.35	1.52
23	53			0.576	0.601		51.3	59.9	1.57	1.83	1.34	1.57
24	54			0.622	0.631		53.0	57.1	1.53	1.82	1.35	1.61
25	55	5.5	5/16	0.405	0.381	1.25	62.0	77.9	1.73	2.42	1.18	1.62
26	56			0.403	0.398		58.7	77.0	1.76	2.34	1.20	1.58
27	57			0.396	0.407		58.3	76.4	1.66	2.32	1.13	1.59
28	58		1/2	0.582	0.621		86.9	110.5	1.81	2.13	1.36	1.63
29	59			0.575	0.642		101.6	112.0	1.96	2.16	1.47	1.67
30	60			0.555	0.615		94.5	110.7	1.93	2.27	1.43	1.74
								Mean	**1.79**	**2.10**	**1.43**	**1.69**
								Coefficient of variation	**0.14**	**0.15**	**0.13**	**0.11**

Table 3. Results of Cruciform Bend Tests from Current Study

[a] NT = "Non-toughness–rated" (E70T7) welds; T = "toughness–rated" (E70T7-K2) welds.
[b] Load eccentricity length.
[c] Nominal (specified) weld size.
[d] Effective weld size based on average *measured* tension and shear leg dimensions, i.e., $w_{eff} = \sqrt{\dfrac{2}{\left(1/L_{shear}\right)^2 + \left(1/L_{tension}\right)^2}}$
[e] Specified plate (root notch) thickness.
[f] R_{max} = maximum eccentric force observed in experiments.
[g] R_n^{AISC} = predicted strength based on AISC approach.
[h] $R_n^{bearing}$ = predicted strength on alternate approach incorporating bearing.

were measured at eight locations along the length of each test weld (within each specimen), using a fillet weld gage and a caliper gage. These detailed measurements enable a more effective interpretation of the test data with respect to design equations. Figure 8 illustrates the average weld profiles (based on all the measurements for a given assembly) for all the welds. In the figure, average weld profiles from all the assemblies (corresponding to the given weld size) are overlaid on one another. Because welding of the test specimens was performed in the horizontal position, the "shear leg" and the "tension leg" had different dimensions. On average, the "shear leg" of the weld (which attaches to the large outer plate) was 38% longer than the "tension leg" (which attaches to the central plate), although this difference was slightly less pronounced in the ½-in. welds. However, in most cases, the tension leg was at least as large as the specified weld size, whereas the shear leg was on average 44% longer then the specified minimum. It is also interesting to observe the dimple shaped weld profiles for the ½-in. weld assemblies, which are produced by the multiple welding passes. The length of each weld was also measured and, in general, was determined to be within 5% of the nominal 4-in. length. It is important to emphasize that all the comparisons with the predicted values are made based on the measured weld profiles and lengths, rather than the nominal weld sizes.

Figure 7(a) shows a representative photograph of a fractured specimen (shown here for Test 19, 1.75-in. root notch, non-toughness ⁵⁄₁₆-in. weld, 8.5-in. eccentricity). Referring to the figure, the fracture surface consists of a region of initial crack propagation straight ahead of the root notch (i.e., perpendicular to the principal bending stresses), before transitioning to shear type fracture at an angle. Figure 7(b) indicates this schematically. This type of failure surface was also observed for the cruciform tension tests (Kanvinde et al., 2008). In many specimens, fracture did not occur on well-defined planes, and sometimes the fracture plane changed orientation along the length of a single weld. Several measurements were conducted on the fractured specimens. Given the irregularity of the fracture surfaces, these post-fracture measurements are interesting only in a qualitative sense and cannot be directly applied to interpret the effectiveness of design guidelines.

EXPERIMENTAL DATA FROM PREVIOUS INVESTIGATIONS

As discussed previously, two other test programs have investigated the strength of welded joints with out-of-plane eccentricity. In the context of this paper, where a key objective is to examine the effectiveness of current design provisions, it is important to examine these other results to enable a comprehensive evaluation of the current design guidelines. Table 1 summarizes data from these other experimental programs (i.e., Dawe and Kulak, 1972; Beaulieu and Picard, 1985). The data are presented in a similar format as Table 3, wherein the various test parameters are presented, including the joint strength, R_{max}, along with test-to-predicted ratios per the AISC design tables. The data are also represented graphically in figures introduced in the next section. As for the tests presented in the current study, strength predictions for these prior tests are based on the measured material properties and weld profiles.

DISCUSSION OF RESULTS

The results from the present study and prior experimental programs are summarized in Tables 1 and 3. Both these tables include the measured joint strengths, R_{max}, and the test-to-predicted ratios, R_{max}/R_n^{AISC}, where R_n^{AISC} represents the strength calculated per Table 8-4 from the *Steel Construction Manual* (AISC, 2005). As discussed in a previous section, Table 8-4 in the *Manual* is based on the instantaneous center approach employing several assumptions, including (1) the weld load-deformation relationship as outlined in Lesik and Kennedy (1990), (2) no consideration of the plate bearing and the corresponding distribution of stresses in the weld, and (3) no consideration of the effect of the root notch on

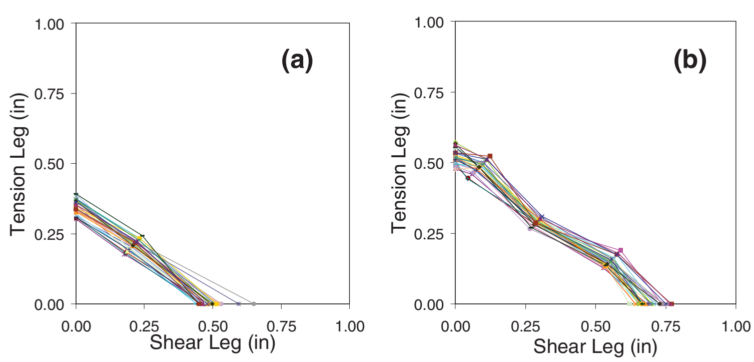

Fig. 8. Mean weld profiles for (a) all the ⁵⁄₁₆-in. welds including the different filler metals and plate thicknesses, and (b) all the ½-in. welds, including the different filler metals and plate thicknesses.

weld ductility. The design table is applied through Equation 6 presented here:

$$R_n^{AISC} = CC_1dL \tag{6}$$

The coefficient C is taken directly from the *Steel Construction Manual* Table 8-4, for different load eccentricity ratios "a" (i.e., ratio of load eccentricity to weld length). The coefficient C_1 accounts for weld strength and is equal to 1.0 for E70XX electrodes. For calculations in the present study, this coefficient is modified to reflect the measured, rather than the nominal material strength. Referring to Table 2, the measured to nominal strength ratios (and hence the C_1 coefficients) for the E70T-7 and E70T7-K2 filler metals are both 1.39. The parameter L is the measured weld length. The parameter d reflects the weld size, indicating the number of sixteenths of an inch in the weld leg size. To reflect the measured weld sizes through this parameter, an effective weld leg dimension is calculated as follows:

$$w_{effective} = \left(\frac{1}{\sqrt{\left(1/L_{shear}\right)^2 + \left(1/L_{tension}\right)^2}} \right) \times \sqrt{2} \tag{7}$$

where the first term reflects the effective throat dimension based on the measured tension and shear leg dimensions of each specimen (averaged over eight measurements along the length of each weld), and the second term ($\sqrt{2}$) reflects the assumed geometrical relationship between the throat size and the effective weld size. Calculating the effective weld size in this manner is consistent with the intent of the AISC design table, such that the weld throat area corresponding to the preceding estimate of effective weld size from Equation 7 corresponds to the weld throat area of the actual specimen, which typically does not have equal leg sizes. The true throat area of the welds may be affected by other factors, such as the number of weld passes (see the irregular weld profile indicated in Figure 8) and weld penetration. However, using these estimates is not consistent with the way in which welds are designed or fabricated. Thus, only the measured leg sizes (rather than measured throat sizes) are used in the calculation of the effective weld size. Once the effective weld size w_{eff} is calculated in inches, the parameter d is conveniently determined through division by (1⁄16).

In addition to Table 1 and Table 3, the comparison between the experimental and predicted strength for all the specimens (including those tested in other studies) is presented graphically in Figure 9 and Figures 10(a)–(d). Figure 9 plots the experimentally measured strength, R_{max}, against the predicted strength, R_n^{AISC}, for all (85) experiments considered. For a closer examination of the trends within the data, Figures 10(a)–(d) plot the test-to-predicted ratios, R_{max}/R_n^{AISC}, against various test parameters, including the load eccentricity, nominal weld size, plate bearing width and weld toughness classification.

Referring to Figure 9, it is immediately apparent that, on average, the AISC design approach predicts strengths significantly lower than the experimental values. Based on all the experiments, the mean value of R_{max}/R_n^{AISC} is 1.75 (coefficient of variation = 0.25). While the AISC approach is significantly conservative for the test results reported in the current study (R_{max}/R_n^{AISC} = 1.94, COV = 0.17), it is relatively less conservative for the other test programs (Dawe and Kulak, 1972; Beaulieu and Picard, 1985) for which the average R_{max}/R_n^{AISC} is 1.15 and 1.32 (COV = 0.12 and 0.21), respectively. This may be attributed to two effects. First, the current study features, on average, larger bearing plate widths (between 1.25 and 2.50 in.), compared to the other test programs (between 0.787 and 1.575 in.). Since the predicted values do not incorporate the effect of bearing, one may argue that the presence of larger bearing widths within a data set may bias R_{max}/R_n^{AISC} ratios within that data set. In fact, referring to Figure 10(a), which plots bearing width versus R_{max}/R_n^{AISC} for all experiments, a general trend is observed such that larger bearing widths result in larger R_{max}/R_n^{AISC} values. When considered in this context, results from the current study appear to be more consistent with the overall trend. Second, the higher R_{max}/R_n^{AISC} values may be attributed to differences in weld metal properties between the current study and the other studies. While the measured strength values for all the studies are incorporated into the predicted strength capacities, recall that the strength estimate implicitly reflects the entire load-deformation response of the weld elements. Thus, the design tables cannot capture the effects of notch toughness (and hence weld ductility) variation between various data sets. Although toughness data (such as Charpy V-Notch energy values) are not documented for the other test programs, it is likely that the current study may result in higher strengths of the joints due to higher weld material toughness as compared to the previous

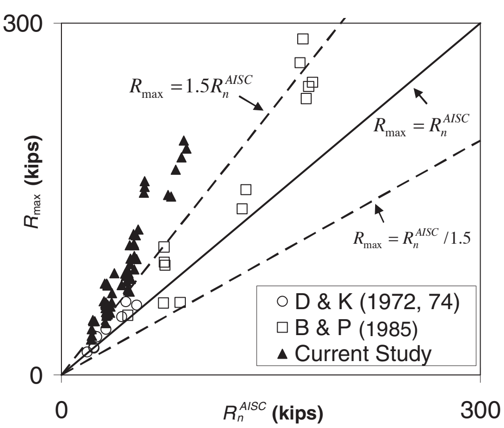

Fig. 9. Comparison between experimental joint strength, R_{max}, and joint strength predicted as per current AISC design table, R_n^{AISC}.

testing programs. However, a detailed comparative analysis (Gomez et al., 2008) between the current (UC Davis) tests and other tests (Ng et al., 2002) indicates that both the filler metals used in the current study are not unusually strong or tough when compared with similar filler metals featured in other recent tests. Thus, results from the current study may be considered only suitable to represent currently used welding materials and practices.

To examine the experimental trends in more detail, Figures 10(a)–(d) plot the R_{max}/R_n^{AISC} ratio against various test parameters for all the experiments. These are now discussed individually:

1. Figure 10(a) plots R_{max}/R_n^{AISC} against the plate bearing width, *t*. A trend is observed across all data sets, such that the predictions become increasingly conservative (i.e., R_{max}/R_n^{AISC} increases) as the bearing thickness of the plates increases. As discussed earlier, this may be explained based on the inability of the design tables to incorporate the effect of bearing on the stress distribution of the welds. It is relevant to note that the bearing thickness is also equal to the weld root notch length. However, based on the data (which shows a consistently increasing trend of R_{max}/R_n^{AISC} with respect to *t*), it appears that the root notch length does not have a significant detrimental effect on the test-to-predicted ratios, especially in the presence of the apparent benefits obtained due to simultaneous increase in bearing thickness. This is consistent with findings from a companion study (Kanvinde et al., 2008) that featured tension tests on cruciform specimens, where the results did not indicate a significant decrease in strength or ductility with an increase in the root notch length above a certain length (typically 1.0 in.).

2. Figure 10(b) plots R_{max}/R_n^{AISC} for all the tests against the weld metal classification. The only tests that feature a weld filler metal with a toughness rating are Tests 31 to 60 of the current study (with the E70T7-K2 filler metal). From the figure, it is evident that, on average, specimens featuring the toughness rated welds have higher R_{max}/R_n^{AISC} values (on average 2.09, COV = 0.15), as compared to the other specimens (on average 1.55, COV = 0.23). As described previously, the AISC design tables reflect a specific weld load-deformation relationship proposed by Lesik and Kennedy (1990), and thus do not distinguish between the tough and non-tough specimens.

3. Figure 10(c) plots R_{max}/R_n^{AISC} versus the eccentricity ratio, *a*, for all the experiments. From the figure, a slight trend is observed within each data set such that increasing the eccentricity ratio reduces the R_{max}/R_n^{AISC} ratios. In the absence of additional data, this trend may be analyzed only in a speculative manner. The specimens with the larger eccentricities result in weld deformations that are more tensile rather than shearing in nature. Although the length of the root notch has been observed to not affect weld strength or ductility when the root notch is longer than about 1 in. (Kanvinde et al., 2008), the *presence* of the transverse root notch produces lower strength and ductility as compared to

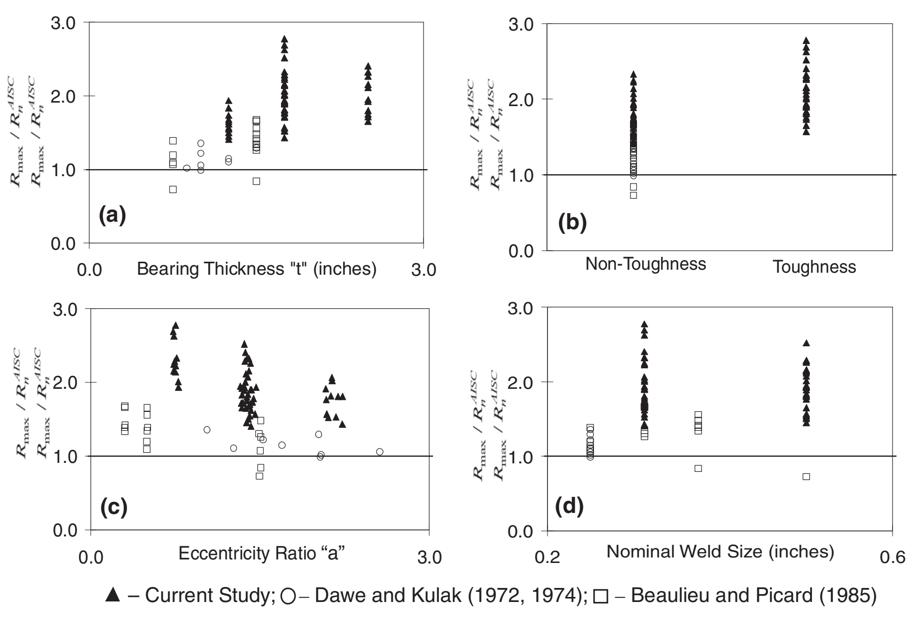

Fig. 10. Effect of various test parameters on the test-predicted ratios, R_{max}/R_n^{AISC}.

lap-joint specimens (where there is no root notch effect). For specimens with a low eccentricity ratio, the deformations are predominantly attributed to shear stresses; thus, the detrimental effect due to the presence of the root notch may be less prominent (i.e., for these connections the root notch is not transverse to the applied stress), as compared to the specimens with the higher eccentricity. In any case, it is important to emphasize that even for the higher eccentricity ratios, the R_{max}/R_n^{AISC} ratios are, on average, greater than 1.0.

4. Finally, referring to Figure 10(d), the weld size did not appear to have a significant influence on the R_{max}/R_n^{AISC} ratios.

In summary, the AISC design tables produce conservative estimates of weld strength for a large majority of the experimental data examined. A reliability analysis of all the experimental data (summarized in Gomez et al., 2008) indicates that the AISC tables, when used in conjunction with a resistance factor $\phi = 0.75$, provide a safety index $\beta = 7.2$, which is well in excess of the target safety index, typically taken as 4.0 for fracture limit states in welded connections. A closer examination of the data reveals that this conservatism may be attributed to two sources. The main issue is that the AISC design tables are based on the IC method, disregarding the effect of plate bearing, which, as discussed previously [and illustrated in Figure 10(a)], has a beneficial influence on the connection capacity. A secondary effect is related to the weld toughness (i.e., ductility). The AISC method implicitly reflects a specific and consistent load-deformation response (and, consequently, ductility) for the weld elements (based on the work on lapped specimens of Lesik and Kennedy (1990). A higher weld ductility than the implicitly assumed values will result in higher R_{max}/R_n^{AISC} ratios. The other effect disregarded by the AISC approach, that is, the existence of the "crack-like" root notch, does not appear to have a prominent effect on strength, especially in the presence of the accompanying benefit on strength due to the increased bearing width.

The next section presents an alternate approach for evaluating the strength of welded connections loaded with out-of-plane eccentricity. By explicitly incorporating bearing in the strength estimates, the aim of this alternate approach is to reduce the conservatism associated with the AISC design tables.

ALTERNATE APPROACH FOR STRENGTH PREDICTION CONSIDERING BEARING

As discussed in the previous section, the AISC design approach predicts the strength of tested welded connections with a high degree of conservatism, providing a safety index well in excess of the target value of 4.0. To address this issue, this section provides an alternate approach to characterize the strength of connections with out-of-plane eccentricity. Referring to the previous section, the AISC standard is conservative mainly due to the omission of the bearing effect between the two connected plates. Fortunately, this effect is convenient to incorporate within the framework of the IC method described previously, by assuming an appropriate stress distribution in the compressive region of the connection. With the objective of developing a refined model for predicting the strength of these joints, several alternative models were applied to the test data and examined for accuracy and consistency. These models included variations based on the IC method (e.g., Dawe and Kulak, 1972) as well as other approaches that resulted in closed form strength equations (e.g., Neis, 1980; Beaulieu and Picard, 1985). The variations in these models resulted from the use of different weld load-deformation relationships (e.g., Butler and Kulak, 1971, or Lesik and Kennedy, 1990) and the assumption of various stress distributions in the compressive bearing region and the tension region. A reliability analysis of all these models, along with a detailed discussion, is presented in Gomez et al. (2008). In the current paper, only one of these models is presented. This model provides the best agreement with the test data, while relying on assumptions that are consistent with the principles of mechanics and weld load-deformation relationships that have been demonstrated to represent measured response.

The model presented in this paper is a modified version of the approach proposed by Dawe and Kulak (1972). In concept, the approach is similar to the one used by AISC (Figure 3), except it explicitly considers bearing stresses in the compressive region of the connection. This is illustrated in Figure 11, which indicates that this method makes use of the instantaneous center of rotation assumptions in the tension zone of the connection and assumes load transfer in the compression zone by bearing of the connected plates and shear of the weld. The normal stress distribution in the compression zone is assumed to be rectangular (i.e., there is no transition from zero stress to yield stress), with the

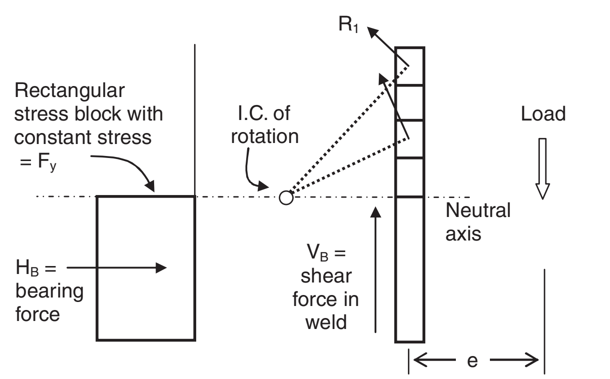

Fig. 11. Assumptions for the alternate method considering bearing.

uniform stress in this region taken as the yield strength of the plate material. As further explained in Gomez et al. (2008), this type of stress distribution reflects typical observations from strain-gaged specimens. Since the normal force in the compression zone (H_B in Figure 11) is carried by bearing between two plates, the weld in this zone is assumed to carry a vertical force, V_B, corresponding to the strength of the weld loaded at an angle, $\theta = 0°$. It is relevant to discuss here that, in general (for more complex connection geometries), the contact between the two connected plates will be nonuniform due to the challenges associated with alignment in a fabricating shop. Thus, a gap may exist between the two connected plates. However, at the ultimate limit state, either the welds in the compression zone will yield, thereby eventually allowing contact, or the plate itself will yield in the compression zone at the toe of the weld. In either case, the assumed stress distribution is consistent with expected response. Thus, the presence of nonuniform contact is not expected to significantly alter the findings of this study.

In the tension region, the weld deformations are determined by applying the principle of the instantaneous center of rotation. Similar to the AISC approach, the corresponding weld load-deformation response is based on Equations 1 through 5 (Lesik and Kennedy, 1990). Finally, the strength capacity is calculated through an iterative procedure similar to the one outlined by Dawe and Kulak (1972) and the AISC approach. The resulting test-to-predicted ratios, $R_{max}/R_n^{bearing}$, for all the specimens are summarized in Table 3 (specimens from current study) and Table 1 (specimens from previous studies). Figures 12 and 13(a)–(d) are equivalent to Figures 9 and 10(a)–(d) discussed in the previous section, but instead feature the predicted strengths, $R_n^{bearing}$, based on the alternate approach that incorporates the bearing effect. Several observations may be made based on Tables 1 and 3 and Figures 12 and 13(a)–(d).

The main observation is that the average test-to-predicted ratio, $R_{max}/R_n^{bearing}$, for all the tests is 1.41 (with a COV = 0.22). This ratio is about 20% lower as compared to the $R_{max}/R_n^{bearing}$ ratios that were obtained disregarding bearing. This suggests that a consideration of bearing produces more accurate estimates of strength. This has important design implications because the method incorporating bearing will result in welds that are significantly smaller compared to those designed as

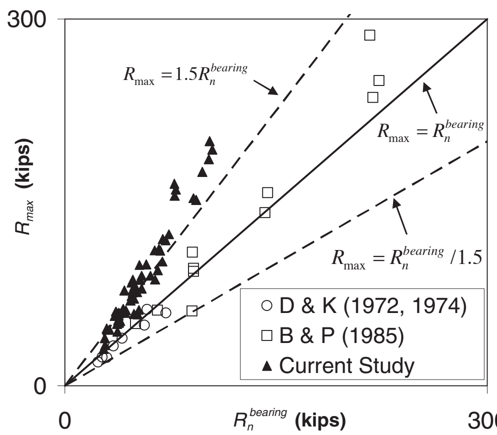

Fig. 12. Comparison between experimental joint strength, R_n, and joint strength predicted using the alternate method incorporating bearing, $R_n^{bearing}$.

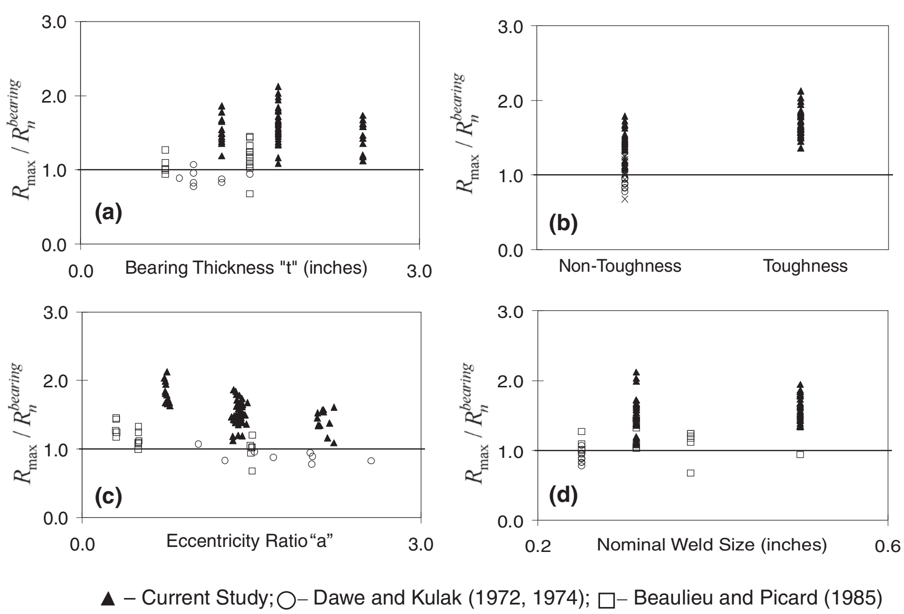

Fig. 13. Effect of various test parameters on the test-predicted ratios, $R_{max}/R_n^{bearing}$.

per the AISC table. A reliability analysis of the data (Gomez et al., 2008) demonstrates that the alternate approach, when used with a capacity factor $\phi = 0.75$, provides a safety index $\beta = 4.6$, which is still in excess of the target safety index $\beta = 4.0$. Since the determination of the weld strengths requires an iterative analysis, the results may be most conveniently presented in the form of a table similar to the current Table 8-4 of the *Steel Construction Manual* (AISC, 2005). Such a table is presented in Gomez et al. (2008).

Figures 13(a)–(d) provide a closer examination of the trends within the experimental data. Comparing Figure 13(a) to Figure 10(a) shown previously, it is apparent that the $R_{max}/R_n^{bearing}$ ratios that incorporate the bearing effect do not show a significant trend with respect to the bearing thickness within any data set. This is encouraging, because it suggests that the alternate method is able to effectively capture the bearing effect. The current tests show higher $R_{max}/R_n^{bearing}$ values on average than the tests from the other test programs, but as discussed previously, this may be attributed to the inherent material toughness of the weld filler metal used in the current study. Refer, for example, to Figure 13(b), that plots the $R_{max}/R_n^{bearing}$ versus toughness classification. Compared to the similar Figure 10(b) shown earlier, a similar trend is observed, such that the approach is on average more conservative for specimens with the toughness rated filler material. In addition to the effect of material toughness, it is relevant to note that that the other test programs had smaller plate thicknesses as compared to the current study. The lower strength observed in these programs may be attributed to weld fracture accompanied by yielding in the base metal, such as may be observed for thinner plates. However Ng et al. (2002) determined that (1) the strength of cruciform tension specimens was not significantly affected by this factor, and (2) this condition (i.e., forcing the base metal to yield before the weld, while ensuring that fracture ultimately occurs in the welds) is difficult to reproduce experimentally, because the exact strength of the weld and base metal is not known at the design stage. Thus, for the current study, thicker plates were chosen to ensure failure in the welds without tension yielding in the base metal. Figures 13(c) and 13(d) plot the $R_{max}/R_n^{bearing}$ ratios against the load eccentricity and the weld size, respectively. The trends observed here are similar to those observed for the AISC approach, and these are not discussed in detail.

It is important to point out that while the alternate method considers the effect of bearing, it does not consider the weld toughness as an input variable. Thus, it cannot distinguish between specimens featuring dissimilar filler metal toughness. The framework of the IC method allows for the convenient implementation of weld toughness, such that the weld load-deformation response (and the fracture deformation Δ_f; refer to Equation 5) may be adjusted to reflect weld toughness. However, incorporating the toughness parameter within the approach is an ambitious goal, given the difficulty in characterizing weld toughness in a quantitative manner and correlating it with the load-deformation capacity of weld elements. Thus, the alternate method described in this paper considers only the most significant effect disregarded by the AISC approach, namely, the bearing between the connected plates. In itself, this has significant cost implications for the design of welds. Possible variations and refinements to the approach described in this section may include (1) explicitly incorporating some measure of weld toughness in the strength prediction, or (2) prescribing different ϕ factors for toughness- or non-toughness-rated specimens, such that a consistent safety index is provided for each type of weld classification. These are described in greater detail in Gomez et al. (2008).

SUMMARY AND CONCLUSIONS

Current design tables (AISC, 2005) for the strength of fillet-welded joints under out-of-plane eccentric loading do not consider two effects that may potentially impact their accuracy. First, they disregard the contribution of bearing between the two connected plates, and second, they do not incorporate the effect of the root notch on weld ductility and strength. The majority of test data that have governed the development of the design tables were obtained from experiments on lapped-splice connections in which neither of these effects are present. This paper presents data from 60 bending tests on cruciform specimens and ancillary tests to investigate the strength of welded connections with an out-of-plane load eccentricity. These specimens feature connections with three different plate bearing thicknesses (1.25, 1.75 and 2.50 in.), two nominal weld sizes (½ in. and 5⁄16 in.), three load eccentricities (3.0, 5.5 and 8.5 in.) and two filler metal classifications ("non-toughness-rated" E70T-7 and "toughness-rated" E70T7-K2). Three replicate tests are conducted for each parameter set. In addition to the tests conducted as part of this study, the analysis of data includes results from other test programs that feature similar experiments.

The experimental results of all documented tests indicate that current design tables (AISC, 2005) are considerably conservative when applied to fillet-welded joints loaded with out-of-plane eccentricity, such that on average, the test-predicted ratio, R_{max}/R_n^{AISC}, is 1.75 (coefficient of variation = 0.25). A closer analysis of the data indicates that this conservatism may be attributed to a bearing mechanism between the connected plates, which is not incorporated in methods used for the development of the AISC design tables. In the presence of this beneficial effect, the accompanying influence of the root notch (whose length is equal to the bearing plate thickness) is minor. The toughness of the filler metal is also determined to contribute to the conservatism of the design approach.

To address these issues, an alternate approach is presented to predict the strength of the welded connections. The approach is similar to the AISC approach (i.e., it is based on the IC method), but it directly incorporates the bearing effect by including an appropriate bearing stress distribution in the compressive region of the connection. Strength predictions based on this approach are significantly less conservative as compared to the AISC approach, such that on average, $R_{max}/R_n^{bearing}$ is determined to be 1.41 (with a COV = 0.22), an approximate 20% decrease with respect to the AISC approach. This has potentially beneficial cost implications since welds designed using the alternate approach will be significantly smaller as compared to welds designed as per the current (AISC) approach. When used with a resistance factor ϕ = 0.75, the alternate approach provides an acceptable safety index β = 4.6. Since application of the alternate approach involves an iterative procedure, the method may be most suitably applied through a design table.

However, the alternate approach does not incorporate all aspects of joint response—especially the weld toughness, which is determined to have an influence on the test-to-predicted ratios. Incorporating the weld toughness as a design parameter may be an ambitious goal, given the subjectivity in characterizing it in a quantitative manner. To incorporate these effects, variations to the method are briefly discussed and refinements are proposed for future work. In addition, the effects of weld profile irregularity cannot be explicitly considered within the scope of this study. For example, the deviation between ideal and true weld profiles, as well as the extent of weld root penetration may have a proportionally dissimilar effect for welds of different sizes. Finally, the results of this study are based on all documented test data on fillet welds with out-of-plane eccentricity. Unfortunately, limited test data (i.e., only three experimental programs) are available for this type of welded detail. There is the possibility of the test data being influenced by unusual material properties or other aspects of the test setup. While the authors have sought to incorporate these effects into their analysis to the extent possible (e.g., by comparing the current test data with other similar data to examine its applicability), the generalization of the results (and possible incorporation into design guidelines) must be accompanied by a fair degree of caution and engineering judgment.

ACKNOWLEDGMENTS

This project was funded by the American Institute of Steel Construction (AISC). The authors gratefully acknowledge Mr. Tom Schlafly of AISC and Dr. Duane Miller of Lincoln Electric, who provided valuable advice and reviewed the welding and shop procedures. Marshall Roberts, graduate student at UC Davis, assisted with the experimental setup, and Jorge Camacho, undergraduate researcher at UC Davis, assisted with the specimen measurements; the authors are thankful for their efforts. The assistance of Mr. David DeBlasio of Gayle Manufacturing Company in preparing the specimens is greatly appreciated. The authors also acknowledge Bill Sluis, laboratory technician at UC Davis, for assistance with design of the test setup.

NOTATION

a = load eccentricity ratio $a = e/L$

A_{throat} = throat area based on average measured leg dimensions

A_w = weld throat area

C = coefficient tabulated in AISC Table 8-4

C_1 = electrode strength coefficient

d = number of sixteenths-of-an-inch of fillet weld size

d_0/d_f = ratio of initial to final (fracture) diameter of tension coupon

e = load eccentricity

$f(\rho)$ = normalized force in the i^{th} weld element

F_{EXX} = electrode tensile strength

F_u = ultimate strength of plate or weld

F_y = yield strength of plate or weld

H_B = normal force in connection compression zone

L = length of weld group

L_{shear}, $L_{tension}$ = mean measured shear and tension leg dimensions, respectively

Nom = nominal (specified) weld size

R_i = resultant force in the i^{th} weld element

R_{max} = experimentally observed maximum strength

R_{ult} = ultimate force of weld element

R_n^{AISC} = strength calculated as per AISC design table

$R_n^{bearing}$ = strength calculated as per the method considering bearing

t = plate bearing width (also equal to nominal root notch length)

V_B = shear force in connection compression zone

w = weld segment leg size

w_{eff} = effective weld size

β = safety index

Δ = deformation of weld element

Δ_f = fracture deformation of weld

Δ_u = deformation of weld at ultimate strength

ε = average true strain across cross section of tension coupon

θ = angle between weld axis and line of action of load

ρ = normalized weld deformation in the i^{th} weld element

ϕ = resistance factor

REFERENCES

AISC (2005), *Steel Construction Manual*, 13th Ed., American Institute of Steel Construction, Chicago.

ASTM E-1820 (2008), "Standard Test Methods for the Measurement of Fracture Toughness," ASTM International, West Conshohocken, PA.

ASTM E-8 (2008), "Standard Test Methods for Tension Testing of Metallic Materials," ASTM International, West Conshohocken, PA.

AWS (2005a), "Specification for Carbon Steel Electrodes for Flux Cored Arc Welding," ANSI/AWS A5.20/A5.20M, American Welding Society, Miami.

AWS (2005b), "Specification for Low-Alloy Steel Electrodes for Flux Cored Arc Welding," ANSI/AWS A5.29/A5.29M, American Welding Society, Miami.

Beaulieu, D. and Picard, A. (1985), "Résultats d'essais sur des assemblages soudés excentriques en flexion (Test Results on Eccentrically Loaded Welded Joints in Bending)," *Canadian Journal of Civil Engineering*, Vol. 12, No. 3, 494–506.

Butler, L.J. and Kulak, G.L. (1971), "Strength of Fillet Welds as a Function of Direction of Load," *Welding Journal, Welding Research Supplement*, Vol. 36, No. 5, 231–234.

Butler, L.J., Pal, S. and Kulak, G.L. (1972), "Eccentrically Loaded Welded Connections," *Journal of the Structural Division,* ASCE, Vol. 98, No. 5, 989–1005.

CISC (2007), *Handbook of Steel Construction,* 9th Ed., Canadian Institute of Steel Construction, Willowdale, Ontario.

Clark, P.J. (1971), "Basis of Design for Fillet-Welded Joints Under Static Loading," *Proceedings, Conference on Improving Welded Product Design*, The Welding Institute, Cambridge, England, Vol. 1, 85–96.

Crawford, S.F. and Kulak, G.L. (1971), "Eccentrically Loaded Bolted Connections," *Journal of the Structural Division,* ASCE, Vol. 97, No. ST3, 765–783.

Dawe, J.L. and Kulak, G.L. (1972), "Behavior of Welded Connections under Combined Shear and Moment," Structural Engineering Report 40, Department of Civil and Environmental Engineering, University of Alberta, Edmonton.

Dawe, J.L. and Kulak, G.L. (1974), "Welded Connections under Combined Shear and Moment," *Journal of the Structural Division,* ASCE, Vol. 100, No. ST4, 727–741.

Gomez, I.R., Kwan, Y.K., Kanvinde, A.M. and Grondin, G.Y. (2008), "Strength and Ductility of Fillet Welds Subjected to Out-of-Plane Bending," Technical Report submitted to the American Institute of Steel Construction, Chicago.

Kanvinde A.M., Gomez I.R., Roberts M., Fell B.V. and Grondin, G.Y, (2008—accepted), "Strength and Ductility of Fillet Welds with Transverse Root Notch," *Journal of Constructional Steel Research,* Elsevier.

Lesik, D.F. and Kennedy, D.J.L. (1990), "Ultimate Strength of Fillet Welded Connections Loaded in Plane," *Canadian Journal of Civil Engineering*, Vol. 17, No. 1, 55–67.

Li, C. (2007), "Reliability Analysis of Concentrically Loaded Fillet Welds," MSc thesis, Department of Civil and Environmental Engineering, University of Alberta, Edmonton, Alberta, October.

Ligtenburg, F.K. (1968), "International Test Series, Final Report. IIW Document XV-242-68," International Institute of Welding.

Miazga, G.S. and Kennedy, D.J.L. (1986), "Behavior of Fillet Welds as a Function of the Angle of Loading," Structural Engineering Report 133, Department of Civil Engineering, University of Alberta, Edmonton.

Miazga, G. S. and Kennedy, D.J.L. (1989), "Behaviour of Fillet Welds as a Function of the Angle of Loading," *Canadian Journal of Civil Engineering*, Vol. 16, No. 4, 583–599.

Neis, V.V. (1980), "Factored Resistance of Welded Connections Subject to Shear and Moment," *Canadian Journal of Civil Engineering*, Vol. 7, No. 1, 84–92.

Ng, A.K.F., Driver, R.G., and Grondin, G.Y. (2002), "Behavior of transverse fillet welds," Structural Engineering Report 245, Department of Civil and Environmental Engineering, University of Alberta, Edmonton.

Pham, L. (1983), "Co-ordinated Testing of Fillet Welds Part 1—Cruciform Specimens—AWRA Contract 94, AWRA Document P6-35-82," *Australian Welding Research*, Vol. 12, 16–25.

Roberts, M. (2008), "Experimental and Analytical Investigations of the Strength and Ductility of Fillet Welds with Transverse Root Notch," Masters Thesis, Department of Civil and Environmental Engineering, University of California, Davis.

Salmon, C.G. and Johnson, J.E. (1996), *Steel Structures, Design and Behavior*, Fourth Edition, Chapter 16, HarperCollins College Publishers, New York.

Sanaei, E. and Kamtekar, A.G. (1988), "Experiments on Some Arbitrarily Loaded Fillet Welds." *Welding Journal*, Welding Research Supplement, Vol. 67, No. 5, 103–109.

Swannell, P. (1981a). "Rational Design of Fillet Weld Groups," *Journal of the Structural Division,* ASCE, Vol. 107, No. ST5, 789–802.

Swannell, P. (1981b). "Weld Group Behavior," *Journal of the Structural Division,* ASCE, Vol. 107, No. ST5, 803–815.

Tide, R.H.R. (1980), "Eccentrically Loaded Weld Groups—AISC Design Tables," *Engineering Journal,* AISC, Vol. 17, No. 4, 90–95.